Skerrett-Byrne David (Orcid ID: 0000-0002-1804-1826)

Fricker Michael (Orcid ID: 0000-0002-8587-1774)

Scott Rodney (Orcid ID: 0000-0001-7724-3404)

Wark Peter (Orcid ID: 0000-0001-5676-6126)

Hansbro Philip (Orcid ID: 0000-0002-4741-3035)

Editorial Office Notes:

RES-21-007.R1

ORIGINAL ARTICLE

Received 4 January 2021

Accepted 14 June 2021

Associate Editor: Judith Mak

Senior Editor: Phan Nguyen

Publication fee waiver: NO

Volume: 26.6-12

Time-resolved proteomic profiling of cigarette smoke-induced experimental chronic obstructive pulmonary disease

David A. Skerrett-Byrne,[1,2,3] Elizabeth G. Bromfield,[2,3,4,] Heather C. Murray,[3,5] M. Fairuz B. Jamaluddin,[3,5] Andrew G. Jarnicki,[1,6] Michael Fricker,[1,3] Ama T. Essilfie,[1,7] Bernadette Jones,[1,3] Tatt J. Haw,[1,3] Daniel Hampsey,[1,3] Amanda L. Anderson,[2,3] Brett Nixon,[2,3] Rodney J. Scott,[3,5] Peter A.B. Wark,[1,3] Matthew D. Dun,[3,5#] Philip M. Hansbro,[1,3,8#]

[1]Priority Research Centre for Healthy Lungs, Hunter Medical Research Institute, Newcastle, NSW, Australia;

[2]Hunter Medical Research Institute, Pregnancy and Reproduction Program, Newcastle, NSW, Australia;

[3]University of Newcastle, Callaghan, NSW, Australia;

[4]Faculty of Veterinary Medicine, Utrecht University, The Netherlands;

[5]Hunter Medical Research Institute, Cancer Research Program, Newcastle, NSW, Australia;

[6]Department of Pharmacology and Therapeutics, University of Melbourne, Parkville, VIC, Australia;

[7]Queensland Institute of Medical Research, Herston, QLD, Australia;

[8]Centre for Inflammation, Centenary Institute and University of Technology Sydney, Sydney, NSW, Australia;

[#]M.D.D. and P.M.H. contributed equally to this work

Correspondence: Philip M. Hansbro, PhD, Centre of Inflammation, Centenary Institute, John's Hopkins Drive, Sydney, NSW 2050, Australia.

Email: p.hansbro@centenary.org.au

Summary at a Glance

Quantitative proteomic profiling of experimental COPD, validated in human lung tissue, identifies protein alterations and defines potential novel clinically-relevant disease drivers, therapeutic targets and biomarkers.

ABSTRACT

Background and objective: Chronic obstructive pulmonary disease (COPD) is the third leading cause of illness and death worldwide. Current treatments aim to control symptoms with none able to reverse disease or stop its progression. We explored the major molecular changes in COPD pathogenesis.

Methods: We employed quantitative label-based proteomics to map the changes in the lung tissue proteome of cigarette smoke-induced experimental COPD that is induced over 8-weeks and progresses over 12-weeks.

Results: Quantification of 7,324 proteins enabled the tracking of changes to the proteome. Alterations in protein expression profiles occurred in the induction phase, with 18 and 16 protein changes at 4- and 6-week time-points, compared to age-matched controls, respectively. Strikingly, 269 proteins had altered expression after 8-weeks when the hallmark pathological features of human COPD emerge, but this dropped to 27 changes at 12-weeks with disease progression. Differentially expressed proteins were validated using other mouse and human COPD bronchial biopsy samples. Major changes in RNA biosynthesis (HNRNPC, MSI2), and modulators of inflammatory responses (S100A1) were notable. Mitochondrial dysfunction and changes in oxidative stress proteins also occurred.

Conclusion: We provide a detailed proteomic profile, identifying proteins associated with the pathogenesis and disease progression of COPD establishing a platform to develop effective new treatment strategies.

Key words: *Experimental chronic obstructive pulmonary disease, emphysema, cigarette smoke, proteomics, therapeutic targets, biomarkers, mouse model*

Short title: Proteomics of experimental COPD

Abbreviations used

CAT	COPD assessment test
COPD:	Chronic obstructive pulmonary disease
CS:	Cigarette smoke
DAMPs:	Damage-associated molecular patterns
DTT:	Dithiothreitol
FDR:	False discovery rate
GOLD:	Global initiative for obstructive lung disease
HILIC:	Hydrophilic interaction liquid chromatography
HNRNPC:	Heterogeneous nuclear ribonucleoproteins C1/C2
IPA:	Ingenuity Pathway Analysis
iTRAQ:	Isobaric tags for relative and absolute quantification
MS:	Mass spectrometry
MSI2:	RNA-binding protein Musashi homolog 2
nLC-MS/MS:	Nano liquid chromatography tandem mass spectrometry
PCA:	Principal component analysis
PRM:	Parallel reaction monitoring
ROS	Reactive oxygen species
S100A1:	Protein S100-A1
TBX:	T-Box

INTRODUCTION

Chronic obstructive pulmonary disease (COPD) is the third leading cause of death globally.[1, 2] It is a complex heterogeneous progressive respiratory disorder, characterized by chronic pulmonary inflammation, progressive airway thickening, and narrowing and destruction of alveoli that all contribute to impaired lung function and severe breathing difficulties.[3, 4] The leading cause is cigarette smoke (CS) inhalation,[2, 5] but air pollution, environmental smoke exposure and genetic factors (e.g. alpha-1 antitrypsin deficiency),[6] are also important instigators in non-smoking patients.[7, 8] The prevalence of COPD continues to rise.[7]

Current treatments for COPD focus on symptomatic control, and are largely unable to halt the progression of disease.[9-11] Despite emerging therapeutics, such as cytokine-receptor antagonists that reduce neutrophil chemotaxis and airway inflammation,[12] there is a critical need to characterize the molecular drivers of COPD. This may identify new therapeutic targets and biomarkers. Analysis of COPD lung tissues has thus far focused on characterizing differences at a genomic and transcriptomic level, however there is little information on the progressive changes in the proteome.[13-17] This limitation is mostly attributed to the large amount of fresh tissue that is required for accurate quantification of protein expression, the requirement for high-level expertise in proteomic-based mass spectrometry (MS) techniques, and accessibility to healthy control tissue.

Given these challenges, sophisticated animal models have been developed and widely used to provide insights into COPD disease pathogenesis with results validated in human tissues.[18-28] These powerful tools provide lung tissues during the development and progression of the hallmark features of COPD that can be investigated in multi-organ systems in reasonable timeframes.[3, 29] We have developed and widely used a mouse model of CS-induced experimental COPD that recapitulates the human clinical features of chronic pulmonary inflammation, airway remodelling

and mucus hypersecretion, emphysema, and impaired lung function in 8-weeks.[26] There, we interrogate this unique model with high resolution quantitative proteomics to characterize the pulmonary proteome during the development and progression of CS-induced COPD. We reveal a critical juncture in the instigation of COPD, where alterations in the machinery responsible for RNA biogenesis and damage-associated molecular patterns (DAMPs) may play important roles in pathogenesis.

METHODS

The ethics statements, mouse model of CS-induced experimental COPD[2, 3, 18, 23, 24, 26, 29-33] and assessment of clinical features (Fig. 1, *A*-*E*), collection of human bronchial biopsies[23, 32] detailed proteomic sample preparation of human endobronchial biopsies, and analysis by parallel reaction monitoring (PRM), bioinformatics, statistical, Ingenuity Pathway Analysis (IPA), and validation by immunohistochemistry are described in detail in Appendix S1 in the Supporting Information .[21, 26, 29, 30, 32-49]

Human subjects

For this study COPD patients were stratified into mild and severe based on the Global Initiative for Obstructive Lung Disease (GOLD) criteria,[2] number of frequent acute exacerbations, and COPD assessment test (CAT) score. Clinical characteristics are summarized in Table 1. The study cohort was comprised of 24 subjects, split into four well-characterized cohorts (n=6 each); healthy controls, healthy smokers, mild (GOLD stage I-II), and severe (GOLD stage III-IV) COPD.

Mouse lung tissue preparation

For each time point (4-, 6-, 8-, 12-week)[26] the hallmark features of COPD were assessed (Fig. 1, *A*-*E*). The lungs of four mice in each group, normal air- or CS-exposed (Fig. 2, *A*), were perfused with tris-buffered saline supplemented with protease (Sigma) and phosphatase inhibitors (Roche, Complete EDTA free), and stored at -80°C until required. Thawed lung tissues were homogenized (100µL ice-cold 0.1M Na_2CO_3 containing protease and phosphatase inhibitors), using the FastPrep-24TM 5G homogenizer (MP Biomedicals, Santa Ana, CA, USA) with the Cool Prep Adaptor. Samples were sonicated (3x10s) and fractionated into membrane-enriched and soluble proteins by ultra-centrifugation (Fig. 2, *B*).[41] Fractions were brought to a concentration of 6M urea, 2M thiourea, reduced with dithiothreitol (10mM DTT), alkylated (20mM iodoacetamide) and digested with 1:30 Lys-C/Trypsin Mix (Promega).[34, 50] Lipids were precipitated from membrane-enriched peptides with formic acid. Peptide populations were purified using desalting columns (Oasis, Waters). Following quantification, peptides (200µg) were labelled using isobaric tags for relative and absolute quantification (iTRAQ) (Fig. 2, *C*),[42] and mixed in a 1:1 ratio. Proteomes were enriched using multi-dimensional strategies,[34, 36, 37, 43, 50] and desalted using modified StageTip microcolumns.[44] Peptides were subjected to offline hydrophilic interaction liquid chromatography (HILIC), and then analysed using high resolution nano liquid chromatography tandem MS (nLC-MS/MS) (Fig. 2, *D*).

Human biopsy preparation

Human endobronchial biopsies were subjected to the same sample preparation methods as mouse samples. However, the protocol was performed without ultra-centrifugation, but with a trichloroacetic acid precipitation step.[51] Following quantification, peptides (30µg) were taken from

each sample and heavy-labeled peptide standards (Table S1 in the Supporting Information) were evenly spiked-in.

LC-MS/MS Analysis

Reverse phase nLC-MS/MS was performed on 9-11 HILIC enriched fractions (Figure S1 in the Supporting Information) for each 8plex, using a Q-Exactive Plus hybrid quadrupole-Orbitrap MS coupled to a Dionex Ultimate 3000RSLC nanoflow high-performance liquid chromatography system (Thermo Fisher Scientific). Samples were loaded onto an Acclaim PepMap100 C18 75 μmx20 mm trap column (Thermo Fisher Scientific) for pre-concentration and online de-salting. Separation was then achieved using an EASY-Spray PepMap C18 75 μmx500 mm column (Thermo Fisher Scientific), employing a linear gradient of acetonitrile (2-25%, 300 nl/min, 125 min). A Q-Exactive Plus MS System was operated in full MS/data dependent acquisition MS/MS mode (data-dependent acquisition). The Orbitrap mass analyser was used at a resolution of 70,000, to acquire full MS with an m/z range of 370–1750, incorporating a target automatic gain control value of $3x10^6$ and maximum fill times of 100ms. The 20 most intense multiply charged precursors were selected for higher-energy collision dissociation fragmentation with a normalized collisional energy of 32. MS/MS fragments were measured at an Orbitrap resolution of 35,000 using an automatic gain control target of $5x10^5$ and maximum fill times of 120ms.

RESULTS

Protein expression patterns underpinning CS-induced experimental COPD

Mice were exposed to CS for 4-12-weeks and progressively developed the hallmark features of COPD including: reduced weight, airway inflammation, emphysema-like alveolar enlargement and impaired lung function (increased total lung capacity, TLC) compared to normal air-exposed mice (Fig. 1, *A*-*E*). Proteomic profiling of lung tissue from mice exposed to CS or air during the induction (4- and 6-weeks) and progression (8- and 12-weeks) phases of experimental COPD,[26] identified 7,324 proteins (FDR≤0.01) across all samples, with an average of 6,034 proteins identified at each time point (see Table 2 and Table S2 in the Supporting Information). Lung tissue was fractionated into membrane-enriched and soluble protein populations to gain insights into spatial and membrane dynamics during different disease phases.[52-54]

Principal component analysis (PCA) revealed a high level of concordance for each lung tissue proteome at each time point (i.e. four mice per treatment, CS- and air-exposed, membrane and soluble enriched for four time points, 4-, 6-, 8- and 12-weeks, Fig. 3, *A*). The distribution of proteins that were identified at each time point are represented in Venn diagrams (Fig. 3, *B*). Notably, ~50% of protein identifications were shared across all time points, while over 16% of proteins were identified exclusively at a single time point. Volcano plots highlight the balance of upregulated and downregulated proteins and their spatial occurrence (Fig. 3, *C*). These data revealed that the most significant changes in the lung proteome induced by CS, occurred at the 8-week time point, where 269 proteins showed significantly altered expression compared to controls (Table S3 in the Supporting Information). This time point is where the chronic clinical features of

COPD first emerge (Fig. 1, *A-E).*[26] Additional PCAs show a clear separation in the proteomic profiles generated from fractionation of lung tissues (Fig. 3, *D*).

Novel proteins linked to pathogenesis

Further assessment of the impact of chronic CS exposure on the lung proteome across the experimental time course identified 2,828 membrane-enriched and 1,176 soluble proteins that had significantly altered expression compared to normal air-exposed controls (ANOVA; FDR<0.05). Unsupervised hierarchical clustering of significantly altered expression profiles identified unique temporal clusters (Table S4 in the Supporting Information), which were assigned biological functions and signalling pathways using Ingenuity Pathway Analysis (Fig. 4, *A* and *B* membrane-enriched and soluble). These analyses implicate mitochondrial dysfunction and oxidative stress (Nrf2, oxidative phosphorylation, AMPK, NADH repair). The membrane-enriched cluster 4 revealed 675 overlapping proteins with increased expression in COPD development (8-week) and progression (12-week) phases. This cluster included eukaryotic initiation factor 2 (EIF2) (*p*-=1.30E-08) and caveolar-mediated endocytosis (*p*=1.49E-08).

Novel proteins linked to different phases of disease

We assigned biological processes and upstream regulators to the progressive phases of disease (Fig. 4, *C* and *D* membrane-enriched and soluble). Analysis of the initial 4-week induction phase in the membrane-enriched fraction, showed altered expression of 434 and 64 proteins linked to apoptosis and necrosis, respectively (Fig. 4, *C*). At this point there were also changes in proteins associated with inhibition of movement of connective tissue (61) and endothelial cells (32),

cytoskeleton formation (72), and microtubule dynamics (209), as well as, adhesion of mast cells (8), necroptosis (30) and morphology (38) and mitochondrial respiration (11).

The expression of these proteins altered as the model transitioned to the 6-week time point. This time point was characterized by activation of immune-related functions including cellular infiltration (105), movement of leukocytes (192) and immune responses of cells (94). Interestingly, the induction phase (4-6-weeks) also featured the enrichment of proteins linked to cellular stress including cell death (121), inflammation (133) and arrested cell movement (388).

In contrast, during disease progression (8-12-weeks) increases were noted in proteins involved in activated functions including apoptosis of endothelial, fibroblast (49) and lung cells (4), generation of reactive oxygen species (ROS) (29), and dysregulated growth (103) and movement of cells (56).

Identification of upstream disease drivers

We next explored upstream regulators and networks using IPA to identify drivers of disease pathogenesis. This analysis demonstrated that lethal-7 (*let-7*) was predicted to be an activated upstream regulator based on alterations observed during the induction phase (4- and 6-weeks) in our proteomic dataset (Fig. 4, *D*). This is of interest as *let-7* is a family of microRNAs, the overexpression of which is linked to delayed tissue repair and reduced movement and proliferation of lung fibroblasts.[55, 56]

Heterogeneous nuclear ribonucleoproteins C1/C2 (HNRNPC) and RNA-binding protein Musashi homolog 2 (MSI2) were amongst the most over-expressed proteins upon disease development (8-weeks, fold change of 12.1 and 3.5, respectively). The damage-associated molecular pattern (DAMP) protein, S100-A1 (S100A1) was also highly overexpressed at this

timepoint (fold change of 5.8). Given these unique changes associated with disease development, the HNRNPC, MSI2, and S100A1 candidates were selected for validation.

Validation of HNRNPC, MSI2, S100A1 as markers of COPD development

To validate the dysregulated protein levels of HNRNPC, MSI2 and S100A1, immunohistochemical analysis was performed using lung sections from the same mice after 8-weeks of CS-exposure compared to air-exposed controls (Fig. 5, *A*). The levels of each of these proteins was significantly increased in the lung sections of CS-exposed mice (Fig. 5, *B*); fold changes of HNRNPC, MSI2 and S100A1 were 2.3 (*t*-test p=0.047), 1.58 (*t*-test p=0.027) and 1.84 (*t*-test p=0.002), respectively. MSI2 and S100A1 were expressed ubiquitously in lung parenchyma but with highest expression noted around the small airways.

HNRNPC, MSI2, S100A1 are overexpressed in patients with COPD

To validate and translate our experimental data to human COPD, we performed targeted proteomics using PRM[34] in human samples (Table S5 in the Supporting Information). Endobronchial biopsies were collected from 24 patients (6 per group) from healthy controls (HC), healthy smokers (HS), mild (MC) and severe COPD (SC) patients (Table 1). PRM analysis of HNRNPC showed a 2.81 (ANOVA p=0.0552) and 3.65 (ANOVA p=0.0067) fold change upregulation in MC and SC patients, respectively, compared to HC (Fig. 5, *C*). Expression of HNRNPC significantly increases in human COPD patients, in line with the 8-week time point in our CS-induce mouse model of COPD (Fig. 5, *D*) showing that our model is valuable as a predictive tool. Interestingly, HNRNPC expression in HS showed no change (fold change -0.13; ANOVA p=0.999) suggesting its expression is not driven by CS-exposure alone. In both HC and

HS, MSI2 and S100A1 were also undetectable. However, MSI2 was detected in both MC and SC, with S100A1 only detected in SC, suggesting potential as targets or biomarkers of both mild and severe stages of human COPD (Fig. 5, *E*).

DISCUSSION

Here, we employed a multi-dimensional enrichment strategy to achieve the first in-depth analysis of the pulmonary tissue proteome during the induction and progression phases of CS-induced experimental COPD, characterizing the profile of 7,324 unique proteins. We focused on the progression phase of COPD, which has not been comprehensively studied. Using ultra-centrifugation with fractionation we performed the first cell compartment enrichment analysis of lung tissue that delineated the contributions of proteins in the membrane versus the cytosol, shedding light on the dynamic interplay between protein abundance and localization in COPD onset.

Two major risk factors driving the pathogenesis of COPD are chronic exposure to CS and age. CS induces cell death through apoptosis, necrosis[57], mitochondrial dysfunction and oxidative stress by inducing the generation of ROS,[58] which all promote persistent lung inflammation.[59] COPD is considered to represent accelerated lung aging[60] involving altered cellular, metabolic and transcriptional changes including, but not limited to, cellular senescence, epigenetic alterations, genomic instability, and telomere attrition.[61-63] Strikingly, after 8-weeks of chronic CS exposure in experimental COPD, the proteomic profiles of lung tissue revealed 269 unique dysregulated proteins, of which 264 were significantly upregulated. All of the chronic pathological features of

human COPD develop at this timepoint including chronic pulmonary inflammation, airway remodeling with mucus hypersecretion, emphysema and impaired lung function.[2-4, 18, 23, 24, 26, 27, 29-33, 58] This timepoint is representative of early GOLD stages 1/2 of COPD,[64] allowing changes to be validated in clinically relevant samples. It is for these reasons that we focused on the progression phase (after 8-weeks) where amongst the 264 upregulated proteins, we identified mitochondrial dysfunction and oxidative stress implicated in pathogenesis, and several novel candidate proteins that potentially play key roles in disease progression; HNRNPC, MSI2 and S100A1.

Proteomic profiling of progressive experimental COPD identified increased expression of proteins involved in RNA biogenesis at 8-weeks. HNRNPC belongs to a family of 20 heterogeneous nuclear ribonucleoproteins with known roles in numerous aspects of RNA biogenesis: regulation of mRNA metabolism, nucleo-cytoplasmic transport, transcription, translation and splicing.[65] Interestingly, HNRNPC is involved in telomerase biogenesis with over-expression inducing telomere shortening.[66] Telomeres are protective DNA caps that reside at the end of chromosomes, limiting DNA degradation and maintaining genomic stability.[67] Longitudinal studies have correlated telomere shortening in lung resident alveolar, endothelial and smooth muscle cells as well as circulating lymphocytes directly with disease severity, impaired lung function and mortality in COPD patients.[67, 68] The correlation with lung function decline was further supported by a meta-analysis of 14 studies.[69] HNRNPC in lung epithelial cells regulates the mRNA stability of urokinase plasminogen activator receptor (uPAR),[70] an emerging biomarker of immune activation and inflammation in COPD.[71, 72] uPAR is strongly linked with pathogenesis, and is upregulated in alveolar wall cells, pulmonary macrophages and small airway epithelia in COPD patients compared to healthy smokers and controls. The upregulation of uPAR significantly correlated with forced expiratory volume in 1 second (FEV_1).[73] It is also implicated in the

destruction of small airways and alveolar cells through the regulation of extracellular matrix degrading enzymes known as the matrix metalloproteinases.[73] Taken together, these observations suggest that the marked upregulation of HNRNPC may promote accelerated ageing of lung tissue known to occur in COPD, and drive the expression of uPAR, which contributes to inflammation and degradation of small airways, thus making it an interesting target for novel therapeutics.

MSI2 is one of two members of the Musashi family of RNA binding proteins, containing two RNA recognition motifs, with regulatory roles in cellular proliferation, determining cell fate, and mRNA translation.[74] There is strong evidence supporting the role of increased cellular senescence in COPD lungs.[60, 63] Senescence is characterized by cells undergoing irreversible replicative arrest,[75] and these processes increase as the lung ages and in COPD.[60] Healthy tissue homeostasis is perturbed by the accumulation of senescent cells, which secrete pro-inflammatory mediators including DAMPs, increasing the generation of ROS, and arresting tissue repair.[60, 75] Using intricate computational algorithms, transcriptional networks were built from publically available gene microarray datasets of diverse human lung epithelial cells.[76] These gene expression profiles revealed the marked suppression of anti-senescence T-Box (TBX) transcription factors coupled with increases in TBX-regulated markers of cellular senescence, suggesting important roles in COPD. These findings were validated in lung tissues from COPD GOLD stage 2-3 patients and healthy smoking subjects (RNA and protein). Amongst the TBX transcription factors identified was TBX-1, which is translationally repressed by over-expression of MSI2 at both genomic and proteomic levels.[77] We observed a 1.8-fold upregulation in the soluble profile of MSI2. This protein was recently shown to be upregulated in non-small cell lung cancer, and to support metastasis by promoting epithelial–mesenchymal transition (EMT) through transforming growth factor beta (TGF-β) signalling and tight junction proteins.[78] Activation of EMT has been

suggested to be a driver of progressive fibrosis and remodelling in the airway epithelium in smokers, but further research is needed to elucidate this relationship.[79, 80] A transcriptome-wide study identified 7,378 distinct gene targets regulated by MSI2 post-transcriptionally, with roles in cell death or survival, DNA repair and replication.[74] Small interfering RNA knockdown of MSI2 demonstrated its regulation of several signalling pathways including epidermal growth factor (EGF), EIF2, hepatocyte growth factor (HGF) and interleukin-6. Both EGF and HGF are regulators of ERK/MAPK, JAK/STAT and P13K/AKT pathways, all orchestrators of inflammation.[81-83] We propose that the marked upregulation of MSI2 at 8-weeks is indicative of its role in inducing clinical features of COPD through the repression of TBX-1 that drives cellular senescence, the modulation of EMT *via* TGF-β signalling and the regulation of inflammatory pathways *via* EGF and HGF signalling. Further mechanistic investigations focused on MSI2 are warranted to elucidate its role in COPD pathogenesis.

In response to injury of resident lung cells DAMPs are released that mediate inflammatory and immune responses to damaged tissue.[84-86] DAMPs are of emerging interest in understanding COPD pathogenesis,[86] since they are potential drivers of innate and adaptive immune responses,[87] but are also strongly implicated in promoting features of ageing.[88] S100 family members have been extensively characterized as DAMPs, with regulatory roles in cell cycle and pro-inflammatory activity.[88] S100A8, S100A9 and S100A12 activate pattern recognition receptors such as Toll-like receptor (TLR)4 and receptor for advanced glycation end-products (RAGE), both driving the activation of nuclear factor-kappaB (NF-κB) signalling,[87] which correlate with airflow limitation and COPD.[31, 89] Upregulation of these factors have been reported in the airways of serve asthma patients,[90] shown to induce mucin-5AC production[91], and in bronchoalveolar fluid of COPD patients.[92] Extracellular S100A1 is internalized *via* caveolin- and clathrin-independent fluid

endocytosis, where it can bind to intracellular TLR4, initiating the formation of a signalling complex of S100A1-TLR4 with the TLR adaptor myeloid differentiation primary response gene-88 (MyD88).[93] This in turn leads to the activation of MAPK and NF-κB pathways, known drivers of inflammation. Previous research from our group has revealed a phenotype of attenuated airway fibrosis and demonstrated a marked reduction in apoptosis, emphysema-like alveolar enlargement, and impaired lung function in *Tlr4*-deficient mice.[31] In the present study we show 2.5 and 0.84 fold increased expression of S100A1 in soluble and membrane-enriched lung profiles, respectively, after 8-weeks of CS exposure. This is coupled with significant enrichment in the IPA analysis of ANOVA significant proteins of canonical pathways involved in caveolar- and clathrin-mediated endocytosis at the same timepoint. TLR signalling is also listed amongst the canonical pathway enrichment, and MyD88 was detected in our membrane-enriched profile. Further, our data indicate that the activation of NF-κB is likely due to abundance changes in 35 known targets (z-score: 1.86) at the 8-week timepoint. In accordance with these findings, previous lung transcriptomic investigation looking five different mouse strains of CS-induced experimental COPD support the active role TLR4 and NF-κB signalling.[94] Moreover, of the 39 transcripts identified in these signalling pathways,[94] 12 are present transiently in our proteomic inventory (see Table S6 in the Supporting Information). Additionally, IPA identified elevated ERK/MAPK signalling with increases in 61 proteins linked to this growth and proliferative signalling pathway detected.

More generally, IPA analysis revealed a significant enrichment in necrosis at every timepoint (Fig. 4, *B* and *D*). S100A1 is also known to interact with RAGE leading to the activation of NF-κB and MAPK signalling pathways.[95] Interestingly, RAGE-deficient mice are protected from CS-induced airway inflammation.[96] Given these data, we propose that S100A1 is an important DAMP

in CS-induced experimental COPD, leading to the activation of NF-κB and MAPK pathways, which in turn contribute to pulmonary inflammation. We have additionally shown S100A1 is expressed in severe COPD patients (Fig. 5, *E*). These data point to S100A1 as a potential therapeutic target upstream of TLR4 and RAGE, which may be targeted to inhibit the progressive features of severe COPD.

The correlation and validation of HRNRPC, MSI2 and S100A1 in clinical human COPD samples highlights their potential roles in the pathogenesis of COPD, and reinforces the clinical relevance of the proteomic profiles detected in our mouse model. Future studies will strengthen our observations by assessing the levels of these factors in the lung tissues of COPD patients with different levels of severity using immunohistochemistry. Importantly, our laboratory has consistently demonstrated that the inhalational exposure of mice to 8-weeks of CS recapitulates the hallmark features of human COPD.[2, 4, 26-28, 30-32, 86, 97] To our knowledge this study represents the most comprehensive CS-induced COPD pulmonary proteome to date. It will serve as an important resource that can be further mined to explore the progressive alterations in the proteome of whole lung tissue. Our mouse model provides unique opportunities to further investigate these candidates mechanistically for the improved understanding of the pathogenesis and therapeutically validate these mediators to develop new treatments and biomarkers for COPD. Future functional studies investigating HRNRPC, MSI2 and S100A1, are needed to elucidate their functional roles in COPD. They may also be relevant to COPD-associated lung cancer.[98]

Acknowledgements

We thank Dr Ben Crossett and Angela Connolly from the Mass Spectrometry Core Facility at The University of Sydney, Nathan Smith from The University of Newcastle Analytical Biomolecular Research Facility (ABRF), Dr Steve Binos from Thermo Fisher Scientific, Matty Bowman and Kristy Wheeldon from The University of Newcastle for technical assistance. Daryl Fitzsimons who assisted with figure design. The Academic and Research Computing Support team, University of Newcastle provided High Performance Computing Infrastructure to support the bioinformatics.

Research funding: PMH is funded by a Fellowship and grants from the National Health and Medical Research Council (NHMRC) of Australia (1079187, 1175134, 1179092, 1156589, 1099095, 1079184). MDD was supported by Cancer Institute NSW, Australia ECF and The University of Newcastle.

Conflict of Interest:

The authors declare that they have no conflicts of interest.

Human Ethics Approval Declaration:

The mouse studies were performed in accordance with the recommendations in the Australian Code of Practice for the Care and Use of Animals for Scientific Purposes issued by the National Health and Medical Research Council of Australia. All protocols were approved by the Animal Care and Ethics Committee of The University of Newcastle in Newcastle, NSW, Australia. All patients provided written informed consent, and experiments with human samples were conducted

in accordance with Hunter New England Area Health Service Ethics Committee (05/08/10/3.09) and University of Newcastle Safety Committee approvals.

Author contributions:

DASB, MDD, PMH conceived and designed the study. DASB, MFBJ, AGJ, MF, ATE, BJ, TJH, DH, and ALA, performed the experiments and data analysis. PABW provided patient samples. DASB prepared the manuscript. EGB, HCM, BN and RJS provided intellectual content. EGB, HCM, AGJ, MF, ATE, BN, RJS, MDD and PMH provided critical revision of the manuscript. PMH funded the study. All authors have read, reviewed and approved the final submitted manuscript

REFERENCES

1 Lozano R, Naghavi M, Foreman K, Lim S, Shibuya K, Aboyans V, Abraham J, Adair T, Aggarwal R, Ahn SY, Alvarado M, Anderson HR, Anderson LM, Andrews KG, Atkinson C, Baddour LM, Barker-Collo S, Bartels DH, Bell ML, Benjamin EJ, Bennett D, Bhalla K, Bikbov B, Bin Abdulhak A, Birbeck G, Blyth F, Bolliger I, Boufous S, Bucello C, Burch M, Burney P, Carapetis J, Chen H, Chou D, Chugh SS, Coffeng LE, Colan SD, Colquhoun S, Colson KE, Condon J, Connor MD, Cooper LT, Corriere M, Cortinovis M, de Vaccaro KC, Couser W, Cowie BC, Criqui MH, Cross M, Dabhadkar KC, Dahodwala N, De Leo D, Degenhardt L, Delossantos A, Denenberg J, Des Jarlais DC, Dharmaratne SD, Dorsey ER, Driscoll T, Duber H, Ebel B, Erwin PJ, Espindola P, Ezzati M, Feigin V, Flaxman AD, Forouzanfar MH, Fowkes FG, Franklin R, Fransen M, Freeman MK, Gabriel SE, Gakidou E, Gaspari F, Gillum RF, Gonzalez-Medina D, Halasa YA, Haring D, Harrison JE, Havmoeller R, Hay RJ, Hoen B, Hotez PJ, Hoy D, Jacobsen KH, James SL, Jasrasaria R, Jayaraman S, Johns N, Karthikeyan G, Kassebaum N, Keren A, Khoo JP, Knowlton LM, Kobusingye O, Koranteng A, Krishnamurthi R, Lipnick M, Lipshultz SE, Ohno SL, Mabweijano J, MacIntyre MF, Mallinger L, March L, Marks GB, Marks R, Matsumori A, Matzopoulos R, Mayosi BM, McAnulty JH, McDermott MM, McGrath J, Mensah GA, Merriman TR, Michaud C, Miller M, Miller TR, Mock C, Mocumbi AO, Mokdad AA, Moran A, Mulholland K, Nair MN, Naldi L, Narayan KM, Nasseri K, Norman P, O'Donnell M, Omer SB, Ortblad K, Osborne R, Ozgediz D, Pahari B, Pandian JD, Rivero AP, Padilla RP, Perez-Ruiz F, Perico N, Phillips D, Pierce K, Pope CA, 3rd, Porrini E, Pourmalek F, Raju M, Ranganathan D, Rehm JT, Rein DB, Remuzzi G, Rivara FP, Roberts T, De Leon FR, Rosenfeld LC, Rushton L, Sacco RL, Salomon JA, Sampson U, Sanman E, Schwebel DC, Segui-Gomez M, Shepard DS, Singh D, Singleton J, Sliwa K, Smith E, Steer A, Taylor JA, Thomas B, Tleyjeh IM, Towbin JA, Truelsen T, Undurraga EA, Venketasubramanian N, Vijayakumar L, Vos T, Wagner GR, Wang M, Wang W, Watt K, Weinstock MA, Weintraub R, Wilkinson JD, Woolf AD, Wulf S, Yeh PH, Yip P, Zabetian A, Zheng ZJ, Lopez AD, Murray CJ, AlMazroa MA, Memish ZA. Global and regional mortality from 235 causes of death for 20 age groups in 1990 and 2010: a systematic analysis for the Global Burden of Disease Study 2010. Lancet (London, England). 2012; **380**: 2095-128.

2 Haw TJ, Starkey MR, Nair PM, Pavlidis S, Liu G, Nguyen DH, Hsu AC, Hanish I, Kim RY, Collison AM, Inman MD, Wark PA, Foster PS, Knight DA, Mattes J, Yagita H, Adcock IM, Horvat JC, Hansbro PM. A pathogenic role for tumor necrosis factor-related apoptosis-inducing ligand in chronic obstructive pulmonary disease. Mucosal Immunol. 2016; **9**: 859-72.

3 Jones B, Donovan C, Liu G, Gomez HM, Chimankar V, Harrison CL, Wiegman CH, Adcock IM, Knight DA, Hirota JA, Hansbro PM. Animal models of COPD: What do they tell us? Respirology. 2017; **22**: 21-32.

4 Keely S, Talley NJ, Hansbro PM. Pulmonary-intestinal cross-talk in mucosal inflammatory disease. Mucosal Immunol. 2012; **5**: 7-18.

5 Eisner MD, Anthonisen N, Coultas D, Kuenzli N, Perez-Padilla R, Postma D, Romieu I, Silverman EK, Balmes JR. An official American Thoracic Society public policy statement: Novel risk factors and the global burden of chronic obstructive pulmonary disease. Am J Respir Crit Care Med. 2010; **182**: 693-718.

6 Hazari YM, Bashir A, Habib M, Bashir S, Habib H, Qasim MA, Shah NN, Haq E, Teckman J, Fazili KM. Alpha-1-antitrypsin deficiency: Genetic variations, clinical manifestations and therapeutic interventions. Mutat Res. 2017; **773**: 14-25.

7 Bilano V, Gilmour S, Moffiet T, d'Espaignet ET, Stevens GA, Commar A, Tuyl F, Hudson I, Shibuya K. Global trends and projections for tobacco use, 1990-2025: an analysis of smoking indicators from the WHO Comprehensive Information Systems for Tobacco Control. Lancet (London, England). 2015; **385**: 966-76.

8 Lopez AD, Shibuya K, Rao C, Mathers CD, Hansell AL, Held LS, Schmid V, Buist S. Chronic obstructive pulmonary disease: current burden and future projections. The European respiratory journal. 2006; **27**: 397-412.

9 Barnes PJ. Corticosteroid resistance in patients with asthma and chronic obstructive pulmonary disease. The Journal of allergy and clinical immunology. 2013; **131**: 636-45.

10 Cazzola M, Page C. Long-acting bronchodilators in COPD: where are we now and where are we going? Breathe. 2014; **10**: 110-20.

11 Spina D. Pharmacology of novel treatments for COPD: are fixed dose combination LABA/LAMA synergistic? European clinical respiratory journal. 2015; **2**.

12 Rennard SI, Dale DC, Donohue JF, Kanniess F, Magnussen H, Sutherland ER, Watz H, Lu S, Stryszak P, Rosenberg E, Staudinger H. CXCR2 Antagonist MK-7123. A Phase 2 Proof-of-Concept Trial for Chronic Obstructive Pulmonary Disease. Am J Respir Crit Care Med. 2015; **191**: 1001-11.

13 Obeidat M, Hao K, Bosse Y, Nickle DC, Nie Y, Postma DS, Laviolette M, Sandford AJ, Daley DD, Hogg JC, Elliott WM, Fishbane N, Timens W, Hysi PG, Kaprio J, Wilson JF, Hui J, Rawal R, Schulz H, Stubbe B, Hayward C, Polasek O, Jarvelin MR, Zhao JH, Jarvis D, Kahonen M, Franceschini N, North KE, Loth DW, Brusselle GG, Smith AV, Gudnason V, Bartz TM, Wilk JB, O'Connor GT, Cassano PA, Tang W, Wain LV, Soler Artigas M, Gharib SA, Strachan DP, Sin DD, Tobin MD, London SJ, Hall IP, Pare PD. Molecular mechanisms underlying variations in lung function: a systems genetics analysis. The Lancet Respiratory medicine. 2015; **3**: 782-95.

14 Pillai SG, Ge D, Zhu G, Kong X, Shianna KV, Need AC, Feng S, Hersh CP, Bakke P, Gulsvik A, Ruppert A, Lodrup Carlsen KC, Roses A, Anderson W, Rennard SI, Lomas DA, Silverman EK, Goldstein DB. A genome-wide association study in chronic obstructive pulmonary disease (COPD): identification of two major susceptibility loci. PLoS genetics. 2009; **5**: e1000421.

15 Sauler M, Lamontagne M, Finnemore E, Herazo-Maya JD, Tedrow J, Zhang X, Morneau JE, Sciurba F, Timens W, Pare PD, Lee PJ, Kaminski N, Bosse Y, Gomez JL. The DNA repair transcriptome in severe COPD. The European respiratory journal. 2018; **52**.

16 Hardin M, Silverman EK. Chronic Obstructive Pulmonary Disease Genetics: A Review of the Past and a Look Into the Future. Chronic obstructive pulmonary diseases (Miami, Fla). 2014; **1**: 33-46.

17 Obeidat M, Dvorkin-Gheva A, Li X, Bosse Y, Brandsma CA, Nickle DC, Hansbro PM, Faner R, Agusti A, Pare PD, Stampfli MR, Sin DD. The Overlap of Lung Tissue Transcriptome of Smoke Exposed Mice with Human Smoking and COPD. Sci Rep. 2018; **8**: 11881.

18 Starkey MR, Plank MW, Casolari P, Papi A, Pavlidis S, Guo Y, Cameron GJ, Haw TJ, Tam A, Obiedat Me. IL-22 and its receptors are increased in human and experimental COPD and contribute to pathogenesis. European Respiratory Journal. 2019: 1800174.

19 Chen-Yu Hsu A, Starkey MR, Hanish I, Parsons K, Haw TJ, Howland LJ, Barr I, Mahony JB, Foster PS, Knight DA. Targeting PI3K-p110α suppresses influenza virus infection in chronic obstructive pulmonary disease. American journal of respiratory and critical care medicine. 2015; **191**: 1012-23.

20 Hansbro PM, Hamilton MJ, Fricker M, Gellatly SL, Jarnicki AG, Zheng D, Frei SM, Wong GW, Hamadi S, Zhou S. Importance of mast cell Prss31/transmembrane tryptase/tryptase-γ in lung function and experimental chronic obstructive pulmonary disease and colitis. Journal of Biological Chemistry. 2014; **289**: 18214-27.

21 Haw T, Starkey M, Nair P, Pavlidis S, Liu G, Nguyen D, Hsu A, Hanish I, Kim R, Collison A. A pathogenic role for tumor necrosis factor-related apoptosis-inducing ligand in chronic obstructive pulmonary disease. Mucosal immunology. 2016; **9**: 859.

22 Haw TJ, Starkey MR, Pavlidis S, Fricker M, Arthurs AL, Nair PM, Liu G, Hanish I, Kim RY, Foster PS. Toll-like receptor 2 and 4 have opposing roles in the pathogenesis of cigarette smoke-induced chronic obstructive pulmonary disease. American Journal of Physiology-Lung Cellular and Molecular Physiology. 2017; **314**: L298-L317.

23 Hsu AC, Dua K, Starkey MR, Haw T-J, Nair PM, Nichol K, Zammit N, Grey ST, Baines KJ, Foster PS. MicroRNA-125a and-b inhibit A20 and MAVS to promote inflammation and impair antiviral response in COPD. JCI insight. 2017; **2**.

24 Fricker M, Goggins BJ, Mateer S, Jones B, Kim RY, Gellatly SL, Jarnicki AG, Powell N, Oliver BG, Radford-Smith G. Chronic cigarette smoke exposure induces systemic hypoxia that drives intestinal dysfunction. JCI insight. 2018; **3**.

25 Donovan C, Starkey MR, Kim RY, Rana BM, Barlow JL, Jones B, Haw TJ, Mono Nair P, Budden K, Cameron GJ. Roles for T/B lymphocytes and ILC2s in experimental chronic obstructive pulmonary disease. Journal of leukocyte biology. 2019; **105**: 143-50.

26 Beckett EL, Stevens RL, Jarnicki AG, Kim RY, Hanish I, Hansbro NG, Deane A, Keely S, Horvat JC, Yang M, Oliver BG, van Rooijen N, Inman MD, Adachi R, Soberman RJ, Hamadi S, Wark PA, Foster PS, Hansbro PM. A new short-term mouse model of chronic obstructive pulmonary disease identifies a role for mast cell tryptase in pathogenesis. J Allergy Clin Immunol. 2013; **131**: 752-62.

27 Nair PM, Starkey MR, Haw TJ, Liu G, Collison AM, Mattes J, Wark PA, Morris JC, Verrills NM, Clark AR, Ammit AJ, Hansbro PM. Enhancing tristetraprolin activity reduces the severity of cigarette smoke-induced experimental chronic obstructive pulmonary disease. Clin Transl Immunology. 2019; **8**: e01084.

28 Starkey MR, Plank MW, Casolari P, Papi A, Pavlidis S, Guo Y, Cameron GJM, Haw TJ, Tam A, Obiedat M, Donovan C, Hansbro NG, Nguyen DH, Nair PM, Kim RY, Horvat JC, Kaiko GE, Durum SK, Wark PA, Sin DD, Caramori G, Adcock IM, Foster PS, Hansbro PM. IL-22 and its receptors are increased in human and experimental COPD and contribute to pathogenesis. Eur Respir J. 2019; **54**.

29 Fricker M, Deane A, Hansbro PM. Animal models of chronic obstructive pulmonary disease. Expert opinion on drug discovery. 2014; **9**: 629-45.

30 Hansbro PM, Hamilton MJ, Fricker M, Gellatly SL, Jarnicki AG, Zheng D, Frei SM, Wong GW, Hamadi S, Zhou S, Foster PS, Krilis SA, Stevens RL. Importance of mast cell Prss31/transmembrane tryptase/tryptase-gamma in lung function and experimental chronic obstructive pulmonary disease and colitis. J Biol Chem. 2014; **289**: 18214-27.

31 Haw TJ, Starkey MR, Pavlidis S, Fricker M, Arthurs AL, Nair PM, Liu G, Hanish I, Kim RY, Foster PS, Horvat JC, Adcock IM, Hansbro PM. Toll-like receptor 2 and 4 have opposing roles in the pathogenesis of cigarette smoke-induced chronic obstructive pulmonary disease. Am J Physiol Lung Cell Mol Physiol. 2018; **314**: L298-l317.

32 Hsu AC, Starkey MR, Hanish I, Parsons K, Haw TJ, Howland LJ, Barr I, Mahony JB, Foster PS, Knight DA, Wark PA, Hansbro PM. Targeting PI3K-p110alpha Suppresses Influenza Virus Infection in Chronic Obstructive Pulmonary Disease. Am J Respir Crit Care Med. 2015; **191**: 1012-23.

33 Liu G, Cooley MA, Jarnicki AG, Hsu AC, Nair PM, Haw TJ, Fricker M, Gellatly SL, Kim RY, Inman MD, Tjin G, Wark PA, Walker MM, Horvat JC, Oliver BG, Argraves WS, Knight DA, Burgess JK, Hansbro PM. Fibulin-1 regulates the pathogenesis of tissue remodeling in respiratory diseases. JCI Insight. 2016; **1**.

34 Degryse S, de Bock CE, Demeyer S, Govaerts I, Bornschein S, Verbeke D, Jacobs K, Binos S, Skerrett-Byrne DA, Murray HC, Verrills NM, Van Vlierberghe P, Cools J, Dun MD. Mutant JAK3 phosphoproteomic profiling predicts synergism between JAK3 inhibitors and MEK/BCL2 inhibitors for the treatment of T-cell acute lymphoblastic leukemia. Leukemia. 2018; **32**: 788-800.

35 Dun MD, Chalkley RJ, Faulkner S, Keene S, Avery-Kiejda KA, Scott RJ, Falkenby LG, Cairns MJ, Larsen MR, Bradshaw RA, Hondermarck H. Proteotranscriptomic Profiling of 231-BR Breast Cancer Cells: Identification of Potential Biomarkers and Therapeutic Targets for Brain Metastasis. Mol Cell Proteomics. 2015; **14**: 2316-30.

36 Nixon B, De Iuliis GN, Hart HM, Zhou W, Mathe A, Bernstein I, Anderson AL, Stanger SJ, Skerrett-Byrne DA, Jamaluddin MFB, Almazi JG, Bromfield EG, Larsen MR, Dun MD. Proteomic profiling of mouse epididymosomes reveals their contributions to post-testicular sperm maturation. Mol Cell Proteomics. 2018.

37 Nixon B, Johnston SD, Skerrett-Byrne DA, Anderson AL, Stanger SJ, Bromfield EG, Martin JH, Hansbro PM, Dun MD. Proteomic profiling of crocodile spermatozoa refutes the tenet that post-testicular maturation is restricted to mammals. Mol Cell Proteomics. 2018.

38 Nair PM, Starkey MR, Haw TJ, Liu G, Horvat JC, Morris JC, Verrills NM, Clark AR, Ammit AJ, Hansbro PM. Targeting PP2A and proteasome activity ameliorates features of allergic airway disease in mice. Allergy. 2017; **72**: 1891-903.

39 Horvat JC, Beagley KW, Wade MA, Preston JA, Hansbro NG, Hickey DK, Kaiko GE, Gibson PG, Foster PS, Hansbro PM. Neonatal chlamydial infection induces mixed T-cell responses that drive allergic airway disease. Am J Respir Crit Care Med. 2007; **176**: 556-64.

40 Eidelman DH, Ghezzo H, Kim WD, Cosio MG. The destructive index and early lung destruction in smokers. Am Rev Respir Dis. 1991; **144**: 156-9.

41 Fujiki Y, Hubbard AL, Fowler S, Lazarow PB. Isolation of intracellular membranes by means of sodium carbonate treatment: application to endoplasmic reticulum. J Cell Biol. 1982; **93**: 97-102.

42 Ross PL, Huang YN, Marchese JN, Williamson B, Parker K, Hattan S, Khainovski N, Pillai S, Dey S, Daniels S, Purkayastha S, Juhasz P, Martin S, Bartlet-Jones M, He F, Jacobson A, Pappin DJ. Multiplexed protein quantitation in Saccharomyces cerevisiae using amine-reactive isobaric tagging reagents. Mol Cell Proteomics. 2004; **3**: 1154-69.

43 Engholm-Keller K, Birck P, Storling J, Pociot F, Mandrup-Poulsen T, Larsen MR. TiSH--a robust and sensitive global phosphoproteomics strategy employing a combination of TiO2, SIMAC, and HILIC. J Proteomics. 2012; **75**: 5749-61.

44 Larsen MR, Cordwell SJ, Roepstorff P. Graphite powder as an alternative or supplement to reversed-phase material for desalting and concentration of peptide mixtures prior to matrix-assisted laser desorption/ionization-mass spectrometry. Proteomics. 2002; **2**: 1277-87.

45 MacLean B, Tomazela DM, Shulman N, Chambers M, Finney GL, Frewen B, Kern R, Tabb DL, Liebler DC, MacCoss MJ. Skyline: an open source document editor for creating and analyzing targeted proteomics experiments. Bioinformatics. 2010; **26**: 966-8.

46 Tyanova S, Temu T, Sinitcyn P, Carlson A, Hein MY, Geiger T, Mann M, Cox J. The Perseus computational platform for comprehensive analysis of (prote)omics data. Nat Methods. 2016; **13**: 731-40.

47 Kramer A, Green J, Pollard J, Jr., Tugendreich S. Causal analysis approaches in Ingenuity Pathway Analysis. Bioinformatics. 2014; **30**: 523-30.

48 Faulkner S, Roselli S, Demont Y, Pundavela J, Choquet G, Leissner P, Oldmeadow C, Attia J, Walker MM, Hondermarck H. ProNGF is a potential diagnostic biomarker for thyroid cancer. Oncotarget. 2016; **7**: 28488-97.

49 Bankhead P, Loughrey MB, Fernandez JA, Dombrowski Y, McArt DG, Dunne PD, McQuaid S, Gray RT, Murray LJ, Coleman HG, James JA, Salto-Tellez M, Hamilton PW. QuPath: Open source software for digital pathology image analysis. Sci Rep. 2017; **7**: 16878.

50 Skerrett-Byrne DA, Trigg NA, Bromfield EG, Dun MD, Bernstein IR, Anderson AL, Stanger SJ, MacDougall LA, Lord T, Aitken RJ, Roman SD, Robertson SA, Nixon B, Schjenken JE. Proteomic dissection of the impact of environmental exposures on mouse seminal vesicle function. Mol Cell Proteomics. 2021: 100107.

51 Zhao X, Huffman KE, Fujimoto J, Canales JR, Girard L, Nie G, Heymach JV, Wistuba, II, Minna JD, Yu Y. Quantitative Proteomic Analysis of Optimal Cutting Temperature (OCT) Embedded Core-Needle Biopsy of Lung Cancer. Journal of the American Society for Mass Spectrometry. 2017; **28**: 2078-89.

52 Ahrman E, Hallgren O, Malmstrom L, Hedstrom U, Malmstrom A, Bjermer L, Zhou XH, Westergren-Thorsson G, Malmstrom J. Quantitative proteomic characterization of the lung extracellular matrix in chronic obstructive pulmonary disease and idiopathic pulmonary fibrosis. Journal of proteomics. 2018; **189**: 23-33.

53 Schiller HB, Fernandez IE, Burgstaller G, Schaab C, Scheltema RA, Schwarzmayr T, Strom TM, Eickelberg O, Mann M. Time- and compartment-resolved proteome profiling of the extracellular niche in lung injury and repair. Molecular Systems Biology. 2015; **11**.

54 Schiller HB, Mayr CH, Leuschner G, Strunz M, Staab-Weijnitz C, Preisendorfer S, Eckes B, Moinzadeh P, Krieg T, Schwartz DA, Hatz RA, Behr J, Mann M, Eickelberg O. Deep Proteome Profiling Reveals Common Prevalence of MZB1-Positive Plasma B Cells in Human Lung and Skin Fibrosis. American journal of respiratory and critical care medicine. 2017; **196**: 1298-310.

55 Osei ET, Florez-Sampedro L, Timens W, Postma DS, Heijink IH, Brandsma C-A. Unravelling the complexity of COPD by microRNAs: it's a small world after all. European Respiratory Journal. 2015; **46**: 807.

56 Huleihel L, Ben-Yehudah A, Milosevic J, Yu G, Pandit K, Sakamoto K, Yousef H, LeJeune M, Coon TA, Redinger CJ, Chensny L, Manor E, Schatten G, Kaminski N. Let-7d microRNA affects mesenchymal phenotypic properties of lung fibroblasts. American journal of physiology Lung cellular and molecular physiology. 2014; **306**: L534-42.

57 Messner B, Frotschnig S, Steinacher-Nigisch A, Winter B, Eichmair E, Gebetsberger J, Schwaiger S, Ploner C, Laufer G, Bernhard D. Apoptosis and necrosis: two different outcomes of cigarette smoke condensate-induced endothelial cell death. Cell Death Dis. 2012; **3**: e424.

58 Kirkham PA, Barnes PJ. Oxidative stress in COPD. Chest. 2013; **144**: 266-73.

59 Dua K, Malyla V, Singhvi G, Wadhwa R, Krishna RV, Shukla SD, Shastri MD, Chellappan DK, Maurya PK, Satija S, Mehta M, Gulati M, Hansbro N, Collet T, Awasthi R, Gupta G, Hsu A, Hansbro PM. Increasing complexity and interactions of oxidative stress in chronic respiratory diseases: An emerging need for novel drug delivery systems. Chem Biol Interact. 2019; **299**: 168-78.

60 Brandsma C-A, de Vries M, Costa R, Woldhuis RR, Königshoff M, Timens W. Lung ageing and COPD: is there a role for ageing in abnormal tissue repair? European Respiratory Review. 2017; **26**: 170073.

61 López-Otín C, Blasco MA, Partridge L, Serrano M, Kroemer G. The hallmarks of aging. Cell. 2013; **153**: 1194-217.

62 Meiners S, Eickelberg O, Königshoff M. Hallmarks of the ageing lung. European Respiratory Journal. 2015; **45**: 807.

63 Barnes PJ, Baker J, Donnelly LE. Cellular senescence as a mechanism and target in chronic lung diseases. American journal of respiratory and critical care medicine. 2019.

64 Liebler DC, Zimmerman LJ. Targeted Quantitation of Proteins by Mass Spectrometry. Biochemistry. 2013; **52**: 3797-806.

65 Geuens T, Bouhy D, Timmerman V. The hnRNP family: insights into their role in health and disease. Hum Genet. 2016; **135**: 851-67.

66 Fu D, Collins K. Purification of human telomerase complexes identifies factors involved in telomerase biogenesis and telomere length regulation. Mol Cell. 2007; **28**: 773-85.

67 Córdoba-Lanús E, Cazorla-Rivero S, Espinoza-Jiménez A, de-Torres JP, Pajares MJ, Aguirre-Jaime A, Celli B, Casanova CJRR. Telomere shortening and accelerated aging in COPD: findings from the BODE cohort. 2017; **18**: 59.

68 Lee J, Sandford AJ, Connett JE, Yan J, Mui T, Li Y, Daley D, Anthonisen NR, Brooks-Wilson A, Man SFP, Sin DD. The Relationship between Telomere Length and Mortality in Chronic Obstructive Pulmonary Disease (COPD). PLOS ONE. 2012; **7**: e35567.

69 Albrecht E, Sillanpää E, Karrasch S, Alves AC, Codd V, Hovatta I, Buxton JL, Nelson CP, Broer L, Hägg S, Mangino M, Willemsen G, Surakka I, Ferreira MAR, Amin N, Oostra BA, Bäckmand HM, Peltonen M, Sarna S, Rantanen T, Sipilä S, Korhonen T, Madden PAF, Gieger C, Jörres RA, Heinrich J, Behr J, Huber RM, Peters A, Strauch K, Wichmann HE, Waldenberger M, Blakemore AIF, de Geus EJC, Nyholt DR, Henders AK, Piirilä PL, Rissanen A, Magnusson PKE, Viñuela A, Pietiläinen KH, Martin NG, Pedersen NL, Boomsma DI, Spector TD, van Duijn CM, Kaprio J, Samani NJ, Jarvelin M-R, Schulz H. Telomere length in circulating leukocytes is associated with lung function and disease. European Respiratory Journal. 2014; **43**: 983.

70 Shetty S. Regulation of urokinase receptor mRNA stability by hnRNP C in lung epithelial cells. Mol Cell Biochem. 2005; **272**: 107-18.

71 Godtfredsen NS, Jørgensen DV, Marsaa K, Ulrik CS, Andersen O, Eugen-Olsen J, Rasmussen LJHJRR. Soluble urokinase plasminogen activator receptor predicts mortality in exacerbated COPD. 2018; **19**: 97.

72 Desmedt V, Delanghe JR, Speeckaert R, Speeckaert MM. The intriguing role of soluble urokinase receptor in inflammatory diseases AU - Desmedt, S. Critical Reviews in Clinical Laboratory Sciences. 2017; **54**: 117-33.

73 Zhang Y, Xiao W, Jiang Y, Wang H, Xu X, Ma D, Chen H, Wang X. Levels of components of the urokinase-type plasminogen activator system are related to chronic obstructive pulmonary disease parenchymal destruction and airway remodelling. J Int Med Res. 2012; **40**: 976-85.

74 Duggimpudi S, Kloetgen A, Maney SK, Munch PC, Hezaveh K, Shaykhalishahi H, Hoyer W, McHardy AC, Lang PA, Borkhardt A, Hoell JI. Transcriptome-wide analysis uncovers the targets of the RNA-binding protein MSI2 and effects of MSI2's RNA-binding activity on IL-6 signaling. J Biol Chem. 2018; **293**: 15359-69.

75 Kirkland JL, Tchkonia T. Cellular Senescence: A Translational Perspective. EBioMedicine. 2017; **21**: 21-8.

76 Acquaah-Mensah GK, Malhotra D, Vulimiri M, McDermott JE, Biswal S. Suppressed expression of T-box transcription factors is involved in senescence in chronic obstructive pulmonary disease. PLoS Comput Biol. 2012; **8**: e1002597.

77 Sutherland JM, Sobinoff AP, Fraser BA, Redgrove KA, Siddall NA, Koopman P, Hime GR, McLaughlin EA. RNA binding protein Musashi-2 regulates PIWIL1 and TBX1 in mouse spermatogenesis. J Cell Physiol. 2018; **233**: 3262-73.

78 Kudinov AE, Deneka A, Nikonova AS, Beck TN, Ahn Y-H, Liu X, Martinez CF, Schultz FA, Reynolds S, Yang D-H, Cai KQ, Yaghmour KM, Baker KA, Egleston BL, Nicolas E, Chikwem A, Andrianov G, Singh S, Borghaei H, Serebriiskii IG, Gibbons DL, Kurie JM,

Golemis EA, Boumber Y. Musashi-2 (MSI2) supports TGF-β signaling and inhibits claudins to promote non-small cell lung cancer (NSCLC) metastasis. 2016; **113**: 6955-60.

79 Nowrin K, Sohal SS, Peterson G, Patel R, Walters EH. Epithelial-mesenchymal transition as a fundamental underlying pathogenic process in COPD airways: fibrosis, remodeling and cancer. Expert Rev Respir Med. 2014; **8**: 547-59.

80 Eapen MS, Sharma P, Thompson IE, Lu W, Myers S, Hansbro PM, Sohal SS. Heparin-binding epidermal growth factor (HB-EGF) drives EMT in patients with COPD: implications for disease pathogenesis and novel therapies. Lab Invest. 2019; **99**: 150-7.

81 Singh D. P38 inhibition in COPD; cautious optimism. Thorax. 2013; **68**: 705.

82 Yew-Booth L, Birrell MA, Lau MS, Baker K, Jones V, Kilty I, Belvisi MG. JAK–STAT pathway activation in COPD. European Respiratory Journal. 2015; **46**: 843.

83 Bozinovski S, Vlahos R, Hansen M, Liu K, Anderson GP. Akt in the pathogenesis of COPD. Int J Chron Obstruct Pulmon Dis. 2006; **1**: 31-8.

84 Kaczmarek A, Vandenabeele P, Krysko DV. Necroptosis: the release of damage-associated molecular patterns and its physiological relevance. Immunity. 2013; **38**: 209-23.

85 Tang D, Kang R, Coyne CB, Zeh HJ, Lotze MT. PAMPs and DAMPs: signal 0s that spur autophagy and immunity. Immunol Rev. 2012; **249**: 158-75.

86 Kim RY, Pinkerton JW, Gibson PG, Cooper MA, Horvat JC, Hansbro PM. Inflammasomes in COPD and neutrophilic asthma. Thorax. 2015; **70**: 1199-201.

87 Pouwels SD, Heijink IH, ten Hacken NH, Vandenabeele P, Krysko DV, Nawijn MC, van Oosterhout AJ. DAMPs activating innate and adaptive immune responses in COPD. Mucosal Immunology. 2013; **7**: 215.

88 Huang J, Xie Y, Sun X, Zeh HJ, 3rd, Kang R, Lotze MT, Tang D. DAMPs, ageing, and cancer: The 'DAMP Hypothesis'. Ageing Res Rev. 2015; **24**: 3-16.

89 Di Stefano A, Caramori G, Oates T, Capelli A, Lusuardi M, Gnemmi I, Ioli F, Chung KF, Donner CF, Barnes PJ, Adcock IM. Increased expression of nuclear factor-kappaB in bronchial biopsies from smokers and patients with COPD. Eur Respir J. 2002; **20**: 556-63.

90 Lee TH, Chang HS, Bae DJ, Song HJ, Kim MS, Park JS, Jun JA, Lee SY, Uh ST, Kim SH, Park CS. Role of S100A9 in the development of neutrophilic inflammation in asthmatics and in a murine model. Clinical immunology (Orlando, Fla). 2017; **183**: 158-66.

91 Kang JH, Hwang SM, Chung IY. S100A8, S100A9 and S100A12 activate airway epithelial cells to produce MUC5AC via extracellular signal-regulated kinase and nuclear factor-kappaB pathways. Immunology. 2015; **144**: 79-90.

92 Merkel D, Rist W, Seither P, Weith A, Lenter MC. Proteomic study of human bronchoalveolar lavage fluids from smokers with chronic obstructive pulmonary disease by combining surface-enhanced laser desorption/ionization-mass spectrometry profiling with mass spectrometric protein identification. Proteomics. 2005; **5**: 2972-80.

93 Rohde D, Schon C, Boerries M, Didrihsone I, Ritterhoff J, Kubatzky KF, Volkers M, Herzog N, Mahler M, Tsoporis JN, Parker TG, Linke B, Giannitsis E, Gao E, Peppel K, Katus

HA, Most P. S100A1 is released from ischemic cardiomyocytes and signals myocardial damage via Toll-like receptor 4. EMBO Mol Med. 2014; **6**: 778-94.

94 Cabanski M, Fields B, Boue S, Boukharov N, DeLeon H, Dror N, Geertz M, Guedj E, Iskandar A, Kogel U, Merg C, Peck MJ, Poussin C, Schlage WK, Talikka M, Ivanov NV, Hoeng J, Peitsch MC. Transcriptional profiling and targeted proteomics reveals common molecular changes associated with cigarette smoke-induced lung emphysema development in five susceptible mouse strains. Inflamm Res. 2015; **64**: 471-86.

95 Khan MI, Su YK, Zou J, Yang LW, Chou RH, Yu C. S100B as an antagonist to block the interaction between S100A1 and the RAGE V domain. PLoS One. 2018; **13**: e0190545.

96 Chen M, Wang T, Shen Y, Xu D, Li X, An J, Dong J, Li D, Wen F, Chen L. Knockout of RAGE ameliorates mainstream cigarette smoke-induced airway inflammation in mice. Int Immunopharmacol. 2017; **50**: 230-5.

97 Tay HL, Kaiko GE, Plank M, Li J, Maltby S, Essilfie AT, Jarnicki A, Yang M, Mattes J, Hansbro PM, Foster PS. Antagonism of miR-328 increases the antimicrobial function of macrophages and neutrophils and rapid clearance of non-typeable Haemophilus influenzae (NTHi) from infected lung. PLoS Pathog. 2015; **11**: e1004549.

98 Caramori G, Ruggeri P, Mumby S, Ieni A, Lo Bello F, Chimankar V, Donovan C, Ando F, Nucera F, Coppolino I, Tuccari G, Hansbro PM, Adcock IM. Molecular links between COPD and lung cancer: new targets for drug discovery? Expert Opin Ther Targets. 2019; **23**: 539-53.

TABLE 1. Clinical characteristics of study subjects

	Targeted Proteomic Analysis			
	Healthy Controls ***(n=6)***	**Healthy Smokers** ***(n=6)***	**Mild COPD** ***(n=6)***	**Severe COPD** ***(n=6)***
Age (years), mean (SD)	55.5 (9.6)	64.2 (10.1)	69.0 (8.4)	76.7 (8.5)
Male (n) : Female (n)	2 : 4	4 : 2	4 : 2	5 : 1
FEV_1 (%), mean (SD)	97.3 (11.6)	98.2 (13.7)	66.7 (9.0)	40.5 (11.1)
Frequent acute exacerbations	*N/A*	*N/A*	< 2	≥ 2
CAT Score, mean (SD)	*N/A*	*N/A*	9.6 (4.3)	16.5 (5.6)
GOLD Stage	*N/A*	*N/A*	1-2	3-4

CAT, COPD assessment test; *FEV_1*, Forced expiratory volume in one second; *GOLD*, Global initiative for obstructive lung disease

Skerrett-Byrne David (Orcid ID: 0000-0002-1804-1826)

Fricker Michael (Orcid ID: 0000-0002-8587-1774)

Scott Rodney (Orcid ID: 0000-0001-7724-3404)

Wark Peter (Orcid ID: 0000-0001-5676-6126)

Hansbro Philip (Orcid ID: 0000-0002-4741-3035)

TABLE 2. Proteomic profiling summary

	#Proteins				
Timepoint	**Total IDs** Unique peptides ≥ 2	**≥ 1.5 Fold change** t-test $p \leq 0.05$	**≤0.667 Fold change** t-test $p \leq 0.05$	**Unique Protein IDs Overlap**	**Unique Protein IDs Time course**
4-week Membrane	4,628	2	3	5,503	6,220
4-week Soluble	4,715	7	6		
6-week Membrane	4,391	8	1	4,781	
6-week Soluble	3,387	6	1		
8-week Membrane	4,877	162	2	5,235	
8-week Soluble	3,600	102	3		
12-week Membrane	3,379	3	11	4,913	
12-week Soluble	4,543	11	2		

Skerrett-Byrne David (Orcid ID: 0000-0002-1804-1826)

Fricker Michael (Orcid ID: 0000-0002-8587-1774)

Scott Rodney (Orcid ID: 0000-0001-7724-3404)

Wark Peter (Orcid ID: 0000-0001-5676-6126)

Hansbro Philip (Orcid ID: 0000-0002-4741-3035)

FIG 1. Cigarette smoke (CS)-induced experimental COPD. Mice were exposed to CS for 4-, 6-, 8-, and 12-weeks inducing hallmark features of human COPD; **A**, reduced weight gain; **B**, reduced total lung capacity, **C**, increased macrophages (M), neutrophils (N) and lymphocytes (L) in broncho-alveolar lavage fluid; **D-E**, emphysema-like alveolar enlargement (scale bar=100 μm). Data are means±standard error the mean of 4-6 mice/group, **P≤0.01, ***P≤0.001, ****P≤0.0001 compared to other groups indicated.

FIG 2. Quantitative proteomic profiling of cigarette smoke (CS)-induced experimental COPD. **A**, Mice were exposed to CS for 4-, 6-, 8-, and 12-weeks to induce the hallmark features of human COPD; **B**, Extracted lung tissue was homogenized and fractionated into membrane and soluble proteins. **C**, iTRAQ 8plex labelled samples were mixed 1:1, and **D**, proteomes were enriched and analysed on a liquid chromatography-tandem mass spectrometer. **E**, Bioinformatics analysis tools, Proteome Discoverer, Perseus and Ingenuity Pathway Analysis were used to characterize the pulmonary proteome. Partially created with Biorender.com

FIG 3. Quantitative proteomic profiling of cigarette smoke (CS)-induced experimental COPD. **A**, Principal component analysis (PCA) of separated protein populations according to timepoint; 4- (blue circles), 6- (turquoise squares), 8- (orange diamonds), and 12- (red triangles) weeks of cigarette smoke-exposure. **B**, Venn diagrams depict the intersects of membrane-enriched and

soluble datasets at different timepoints. **C**, Volcano plots of each timepoint and fractionation. Dotted lines denote cut-offs of fold change ± 1.5 (x-axis) and student *t*-test significance ≤0.05 (y-axis) **D,** PCA separates protein populations based on fractionation, membrane-enriched (gold squares) and soluble (green circles) fractions at each timepoint.

FIG 4. Protein pathways, networks and functions influenced by cigarette smoke (CS). Hierarchical clustering analysis of ANOVA significant (FDR<0.05) protein expression levels (CS/Control; log2) of **A**, membrane enriched and **B**, soluble populations. Clustering identifies unique clusters with the top five significant canonical pathways and molecular functions listed. **C** and **D**, Hierarchical clustering of activity scores of upstream regulators and downstream biological functions.

FIG 5. Validation and translation of comparative and quantitative proteomics in experimental and human COPD tissue. **A**, Immunohistochemical sections of HNRNPC, MSI2 and S100A1 in mouse lung tissue slices (n=6) and **B**, quantified fold changes (cigarette smoke (CS)/Control; log2) after 8-weeks of chronic CS-exposure; *t*-test with post-hoc Welch's test *P≤0.05, **P≤0.01. **C**, Targeted parallel reaction monitoring (PRM) validation in clinical COPD samples of hnRNP C1/C2 **D**, Proteomic iTRAQ fold changes of targets after 8-weeks of chronic CS-exposure in experimental COPD. **E**, PRM validation MSI2 and S100A1 in clinical COPD samples; One-way ANOVA **P≤0.01

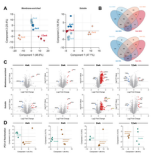

RESP_14111_RESP_14111_Skerrett-Byrne et al. 2021 Respirology Figure 3.tif

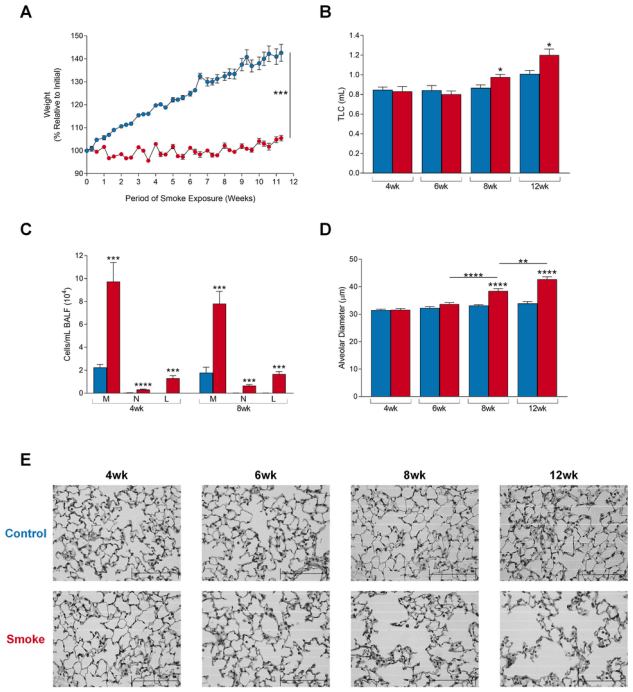

RESP_14111_RESP_14111_Skerrett-Byrne et al. 2021 Respirology R1 Figure 1.tif

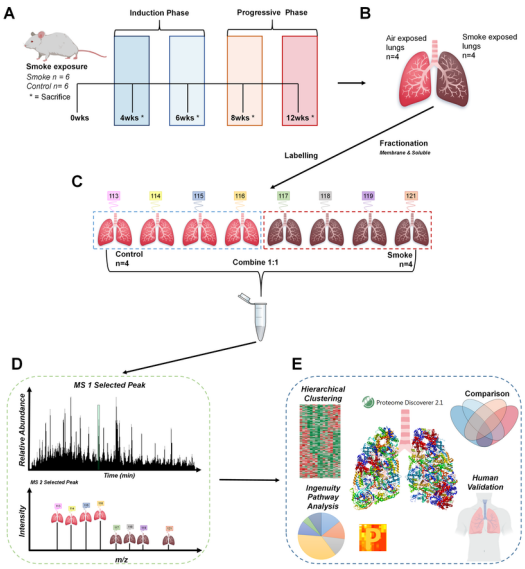

RESP_14111_RESP_14111_Skerrett-Byrne et al. 2021 Respirology R2 Figure 2.tif

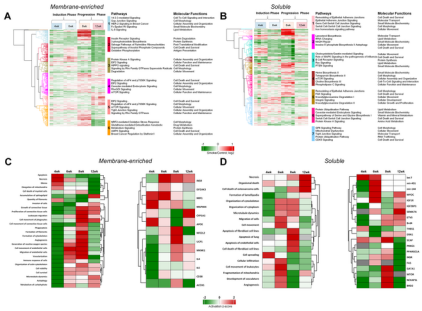

RESP_14111_RESP_14111_Skerrett-Byrne et al. 2021 Respirology R4 Figure 4.tif

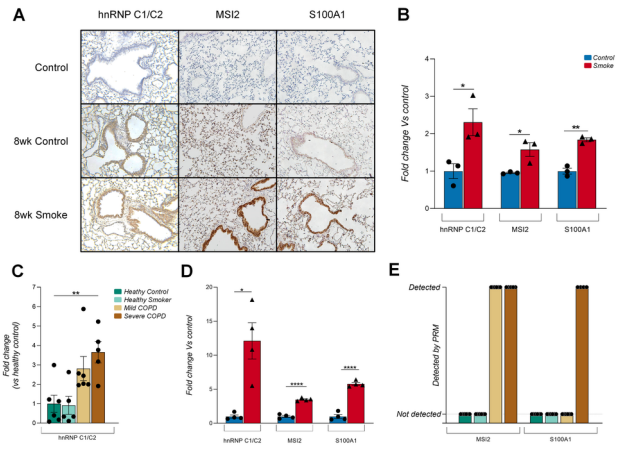

RESP_14111_RESP_14111_Skerrett-Byrne et al. 2021 Respirology R5 Figure 5.tif